Quieting an environmental magnetic field without shielding

Kangda Xiao, Li Wang (iD), Jun Guo, Maohua Zhu, Xiuchao Zhao (iD), Xianping Sun, Chaohui Ye, and Xin Zhou (iD)

View Online   Export Citation   CrossMark

Nanopositioning Systems

Modular Motion Control

AFM and NSOM Instruments
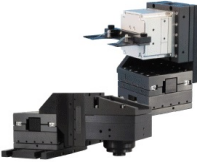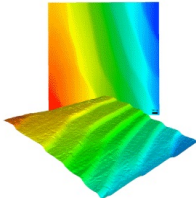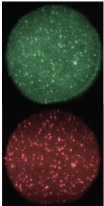
Single Molecule Microscopes

MAD CITY LABS INC.
www.madcitylabs.com

Quieting an environmental magnetic field without shielding

Kangda Xiao,[1,2] Li Wang,[1,2] Jun Guo,[1,2] Maohua Zhu,[1,2] Xiuchao Zhao,[1,2] Xianping Sun,[1,2] Chaohui Ye,[1,2]
and Xin Zhou[1,2,a]

AFFILIATIONS

[1] Key Laboratory of Magnetic Resonance in Biological Systems, State Key Laboratory of Magnetic Resonance and Atomic
and Molecular Physics, National Center for Magnetic Resonance in Wuhan, Wuhan Institute of Physics and Mathematics,
Innovation Academy for Precision Measurement Science and Technology, Chinese Academy of Sciences - Wuhan National
Laboratory for Optoelectronics, Wuhan 430071, People's Republic of China

[2] Innovation Academy for Precision Measurement Science and Technology, University of Chinese Academy of Sciences,
Beijing 100049, People's Republic of China

[a] Author to whom correspondence should be addressed: xinzhou@wipm.ac.cn

ABSTRACT

We construct an active magnetic compensation device and propose an efficient magnetic compensation method that suppresses a wider range of frequencies and amplitudes of time-varying magnetic fields than conventional methods. This system can compensate for all frequencies in the bandwidth of the sensors used by analyzing and extracting the spectral characteristics of the ambient field. We compensate simultaneously for various types of interference in rotation and achieve a reduction of the 50-Hz power-frequency field noise by 36 dB. Meanwhile, the real-time compensation of the field gradient is also investigated. Due to the effectiveness and extensive applicability of this method, it holds great promise for applications in atomic magnetometers, electron microscopes, and atomic clocks.

Published under license by AIP Publishing. https://doi.org/10.1063/5.0007464

I. INTRODUCTION

Atomic magnetometers can measure magnetic fields with ultra-high sensitivity. They can compete with superconducting quantum interference devices (SQUIDs), without the requirement of cryogenics.[1,2] Atomic magnetometers have been widely used in low-field and zero-field nuclear magnetic resonance (NMR)[3–5] and for detecting magnetic particles.[6] Most atomic magnetometers use multiple layers of mu-metal to passively shield the magnetic field noise in the environment.[1,7] This method limits the measurement range of atomic magnetometers, so they cannot be applied to geographical mapping and detecting magnetic anomalies.[8] Therefore, it would be useful to operate atomic magnetometers in unshielded geomagnetic environments.[9,10] However, pseudo-static fields, power-frequency AC field noise, and field gradients in the environment limit the sensitivity of an unshielded magnetometer.[11] In addition, quieting an environmental magnetic field is also a requisite for electron microscopes and atomic clocks.[12,13] Thus, it is important to develop an active magnetic compensation system that can suppress field noise and field gradients.

Some methods have been proposed for canceling field noise and field gradients without using mu-metal shielding, but they have certain limitations. The traditional proportional–integral–differential (PID) method of magnetic compensation is not applicable to high-frequency field noise and various types of interference, as it is limited by the feedback speed of the system.[14] An inductive pickup coil with a feedback amplifier can actively cancel high-frequency field noise, but it is difficult to screen the specific capacitance of the pickup coil.[15] A system consisting of a feedback loop and a feedforward circuit can compensate only for fixed-phase AC field noise, which limits its application in complex magnetic environments.[16]

Herein, we develop a magnetic compensation method that efficiently suppresses the various types of interference in the environment without shielding. First, magnetoresistive sensors are employed to measure the ambient fields. Second, the spectral characteristics of the ambient field are analyzed in real time and information about the various ambient interference sources is extracted. Third, using the relation between the magnetic field and the current in the coils, compensatory currents can be precisely
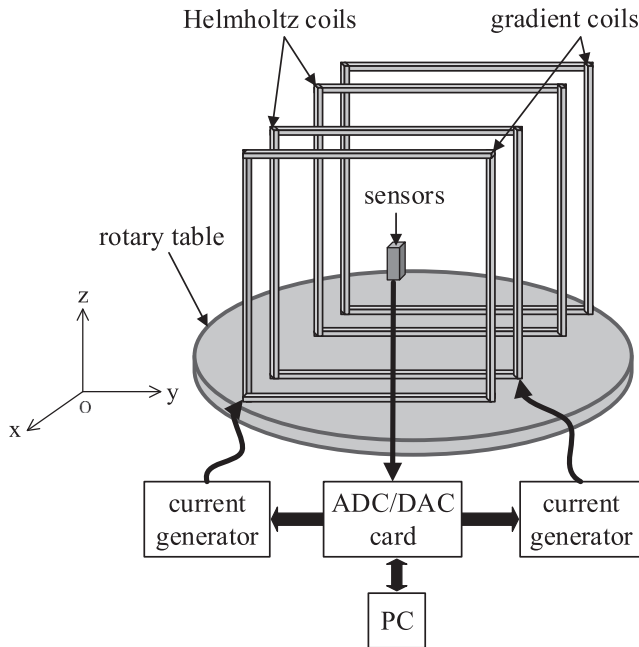
FIG. 1. Schematic of the experimental setup. Only the *x*-axial coils are shown for clarity. The ambient field measured by the magnetoresistive sensors is collected by a 16-bit ADC card and sent to a computer, which performs the spectral analysis. The current generators receive a signal from the DAC card based on the spectral analysis and drive the coils to produce a magnetic field that compensates for the ambient field.

calculated. Finally, the compensation for the various ambient interference sources is achieved by outputting a linear superposition of the calculated currents. In the experiments, a pseudo-static field, power-frequency AC field noise, and field gradient were simultaneously attenuated by 111 dB, 36 dB, and 20 dB, respectively.

II. EXPERIMENTAL SETUP

The experimental setup is shown in Fig. 1, though only the *x*-axial coils are drawn for clarity. The device has square triaxial Helmholtz and gradient coils, which have a length of 350 mm. The relation between the spacing D and the side length L of the gradient coils satisfies $D = 0.9 \times L$. The gradient coils are wired in series. A triaxial magnetoresistive sensor (Honeywell HMC1053) with a size of $7.4 \times 7.4 \times 2.8$ mm^3, which can easily be integrated with an atomic magnetometer, is placed at the center of the coils. The sampling rate is f_s. The bandwidth (in the set/reset mode) and sensitivity of the sensor are 125 Hz and 5 mV/G, respectively. In the center of the Helmholtz coils ($30 \times 30 \times 30$ mm^3), the uniformity of the magnetic field is about 10^{-5}. To measure the field gradients in the *x* and *y* directions, two pairs of sensors are placed symmetrically and parallel to the *x*-axis and *y*-axis, respectively. The sensors in each pair are 30 mm apart. The maximum output of the current generator is 1 A. The noise current (rms, frequency <10 Hz) is about 20 μA, corresponding to a magnetic field noise of about 2 nT. The coils are placed on a non-magnetic one-dimensional rotary table, which is controlled by a stepper motor with an angular resolution of 0.01°.

III. METHOD

Our method consists of three processes: measurement, analysis, and output. The basic principle is shown in Fig. 2. Each process is split into a sequence of blocks of duration τ. The time τ is more than two periods of AC field noise. In the measurement phase, during the nth block, the sensors measure the ambient field $B^{(n)}$, which can be expressed as a one-dimensional array of N elements, $N = \tau/f_s$. In the analysis phase, the spectral characteristics of the data $B^{(n)}$ are analyzed in real time to extract the dominant AC field noise $B_{AC}^{(n)}$ and the pseudo-static field $B_{DC}^{(n)}$. The compensatory currents $I_{AC}^{(n)}$ and $I_{DC}^{(n)}$ can be determined from the coefficient K in the relation between the magnetic field and the current in the coils. Finally, in the output phase, the overall compensatory current $I_{total}^{(n)}$ is the output, which is a linear superposition of $I_{AC}^{(n)}$ and $I_{DC}^{(n)}$.

The magnetic field in the environment includes the AC field noise and a pseudo-static field,

$$B^{(n)} = B_{AC}^{(n)} + B_{DC}^{(n)}. \tag{1}$$

To realize high-precision active magnetic compensation, we need to separate out the dominant field noise $B_{AC}^{(n)}$, which has the frequency f. The amplitude $\left| B_{AC}^{(n)} \right|$ and phase $\theta^{(n)}$ of the separated component are calculated as follows:

$$
\begin{aligned}
a^{(n)} &= \sum_{i=0}^{N-1} B_i^{(n)} \sin\left(\frac{2\pi f i}{f_s} \right), \\
b^{(n)} &= \sum_{i=0}^{N-1} B_i^{(n)} \cos\left(\frac{2\pi f i}{f_s} \right), \\
\left| B_{AC}^{(n)} \right| &= \frac{2\sqrt{\left(a^{(n)}\right)^2 + \left(b^{(n)}\right)^2}}{N}, \\
\theta^{(n)} &= \tan^{-1}\left(\frac{a^{(n)}}{b^{(n)}} \right), \\
B_{AC}^{(n)} &= \left| B_{AC}^{(n)} \right| \sin\left(\frac{2\pi f i}{f_s} + \theta^{(n)} \right).
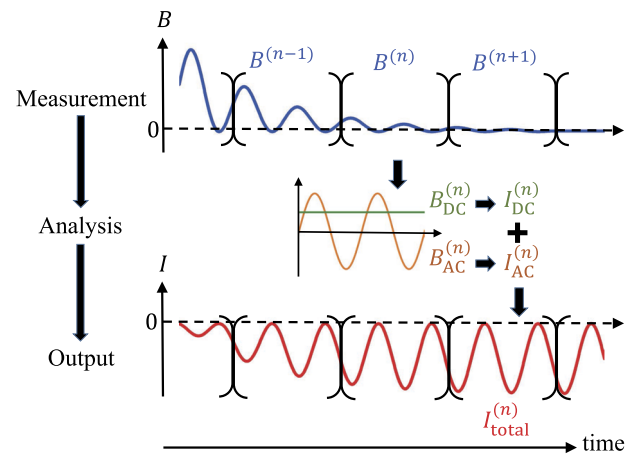\end{aligned}
\tag{2}
$$

FIG. 2. Magnetic compensation. The measurements and output are in the same time reference.

After $B_{AC}^{(n)}$ and $B_{DC}^{(n)}$ have been separately determined, $I_{total}^{(n)}$ can be calculated as follows:

$$I_{total}^{(n)} = I_{AC}^{(n)} + I_{DC}^{(n)}, \qquad (3)$$

where

$$I_{AC}^{(n)} = I_{AC}^{(n-1)} - \frac{\tilde{B}_{AC}^{(n)} - \tilde{B}_{AC}^{(n-1)}}{K}$$

and

$$I_{DC}^{(n)} = I_{DC}^{(n-1)} - \frac{B_{DC}^{(n)} - B_{DC}^{(n-1)}}{K} \cdot damping.$$

We use $\tilde{B}_{AC}^{(n)}$ instead of $B_{AC}^{(n)}$ because there is a phase difference $2\pi f \Delta t$ in time Δt between the sampling and the output. The damping coefficient is mainly used to smooth the spectrum after compensation.

If there is more than one source of frequency noise in the environment, it is necessary only to increase the number of AC field noise terms in Eq. (1). If there is low-frequency field noise, we may need a relatively long time for data acquisition. In this process, the suppression of AC field noise will not be affected because the AC is still output continuously. Under some special cases, such as the existence of pulses or random noise in the environment, we will not extract the AC field noise to enable fast magnetic compensation. The output of the current generator is controlled by the DAC card. The system works in the closed-loop negative-feedback mode.

IV. RESULTS AND DISCUSSION

A. Reduction of field magnitude

The 50-Hz power-frequency AC field noise, which has an amplitude of about 1 mG in our laboratory, can be compensated for well using our system, as shown in Fig. 3. The time τ of hyperfine spectral analysis is 0.1 s. It can be observed that the compensated magnetic field at 50 and 100 Hz is attenuated by 36 dB and 25 dB, respectively. The pseudo-static field can also be compensated for. The total magnetic field after compensation is about 1 ± 15 nT, which is mainly limited by the resolution of the sensors.

Moreover, we theoretically analyzed passive eddy-current shielding for an AC magnetic field. However, it is poor in frequency selectivity for some specific signals and bulky for some applications. The details are given in the supplementary material (Fig. S1 in the supplementary material).

B. Reduction of field gradient

The magnetic field gradient dB_x/dx (dB_y/dy) is obtained from the difference in the magnetic field measured by each sensor in the pair of sensors in the x (y) direction[17] and compensated for by the gradient coils. The process is similar to the reduction of the field magnitude. We did not extract AC field gradient noise from the ambient field gradient because there are no prominent noise peaks in the frequency domain of the field gradient. The field gradients in
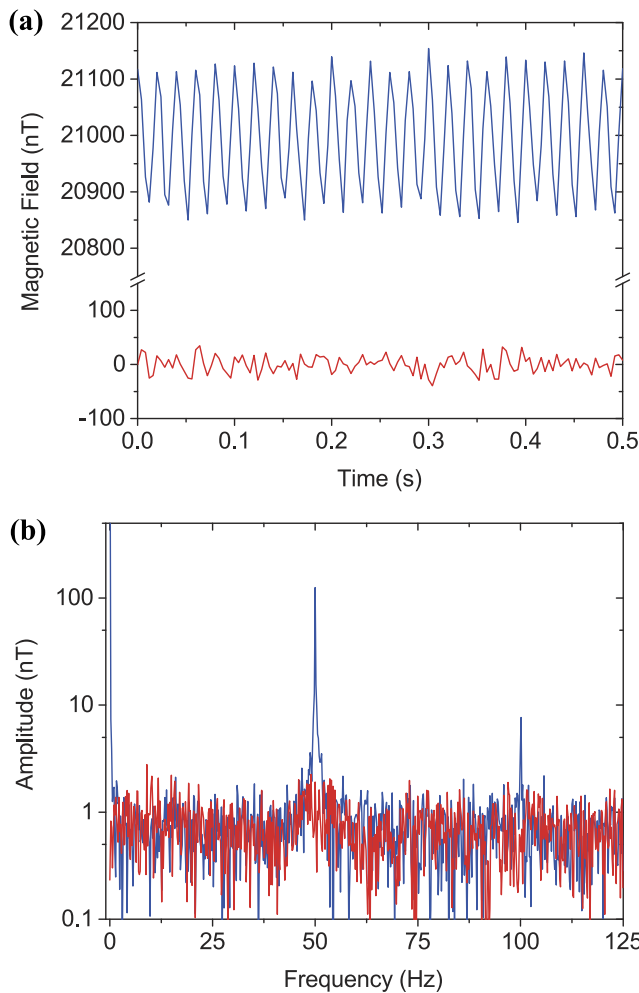

FIG. 3. Compensation for the magnetic field in the x direction. (a) Time domain. (b) Frequency domain. The blue (red) lines are without (with) compensation. The simultaneous compensation of magnetic fields in the y and z directions is also realized (Fig. S2 in the supplementary material).

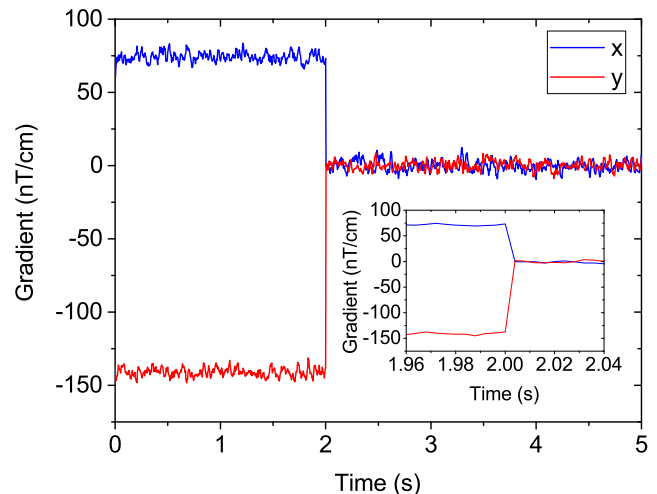

FIG. 4. Compensation for the magnetic field gradients in the x and y directions. The blue (red) line represents the magnetic field gradient in the x (y) direction. The inset is an enlargement for the compensatory time.

the x and y directions were about 74 nT/cm and 141 nT/cm before compensation, respectively. The gradients in the x and y directions produced by the Helmholtz coils are both about 1.3 nT/cm, and the coefficients for the gradient coils in the x and y directions are both about 225 nT/(cm A). The results of the real-time compensation of field gradients in the x and y directions are shown in Fig. 4. The compensatory time is as short as 4 ms (inset of Fig. 4), which is limited by the sampling rate of the sensors. The compensated field gradients are attenuated by more than 20 dB. This method can also compensate for all the other components of a field gradient tensor.

C. Magnetic compensation for various types of interference

Finally, we experimentally realized magnetic compensation while the apparatus was rotating. The rotation speed Ω = 1 rpm.
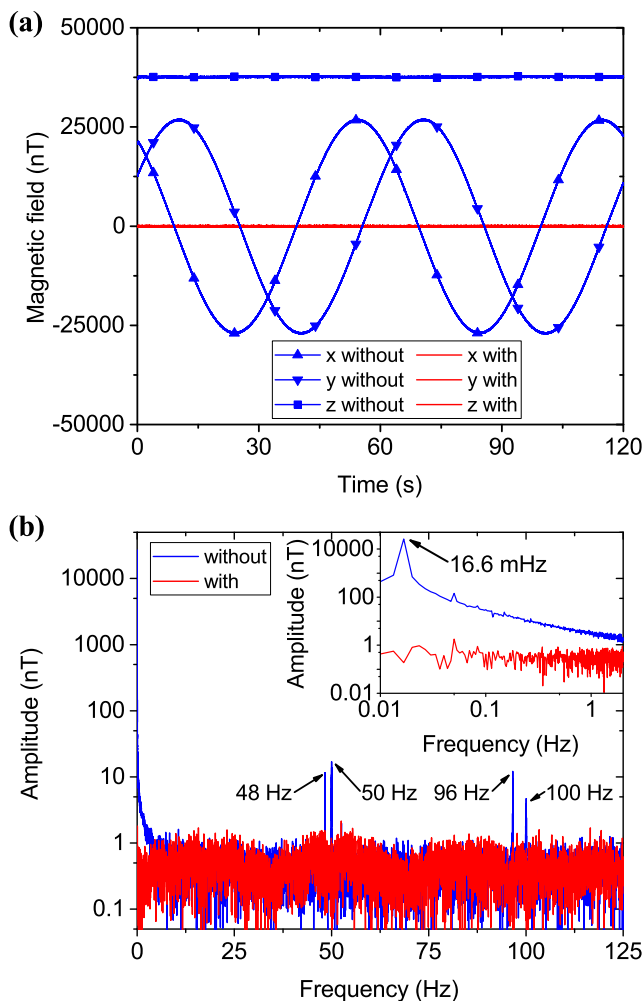

FIG. 5. Compensation for various types of interference during rotation. The blue (red) lines are the magnetic fields without (with) compensation. (a) Time domain of the magnetic field in three directions. (b) Frequency domain of the magnetic field in the x direction. The low-frequency region is plotted in the inset for clarity.

TABLE I. Noise produced by the system.

Noise source	rms noise (nT)
ADC card	4.2
Sensors	12
Current generator	2.1

Figure 5(a) shows the magnetic fields in three directions during rotation. These fields were measured by the central sensor. The horizontal magnetic field was about 243 mG, and the vertical magnetic field was about 370 mG with a perturbation of 200 nT. The perturbation was mainly due to the inclination during rotation. Figure 5(b) shows the frequency domain of the magnetic field in the x direction. After compensation, the magnetic field at $1/\Omega$ = 16.6 mHz disappeared, illustrating that this method can compensate for time-varying magnetic fields with a high amplitude. In addition, the magnetic fields at 48 Hz and 50 Hz and their harmonics have been simultaneously cleared. The magnetic fields at 48 Hz and 96 Hz are generated by the stepper motor of the rotary system. The low-frequency vibration noise was greatly reduced by optimizing the current and pulse per revolution of the stepper motor. These results show that this method not only can compensate well for various types of ambient interference simultaneously but can also be expanded to applications with moving carriers.[18]

Finally, we evaluated the noise produced by the compensation system. The noise consists of three primary parts and is mainly from the sensors (Table I). The 50-Hz electronic noise of the compensation system is about 0.34 nT/$\sqrt{Hz}$, which was measured by placing the sensors in a five-layer mu-metal shield to eliminate the electromagnetic field in the environment (Fig. S3 in the supplementary material).

To improve the magnetic compensation of our system, it could be integrated with an atomic magnetometer as another sensor, due to its sub-fT sensitivity.[19] This would enable the application of this system for pT and even sub-pT measurements.[20] Additionally, if a higher precision current generator[21] and ADC/DAC card were employed, the measurements would be more sensitive.

This method can also be applied to the compensation of magnetic fields with higher frequencies (Fig. S5 in the supplementary material). In addition, a signal of interest can be extracted accurately from external noise even if the external fields are canceled (Fig. S6 in the supplementary material). Thus, the performance of our method is superior to that of the traditional PID method in compensating for higher frequency fields and extracting a signal of interest.

V. CONCLUSIONS

In conclusion, we have developed an active magnetic compensation device and proposed an efficient method for magnetic compensation using spectral analysis. We compensated for field noise and field gradients. The magnetic field was about 1 ± 15 nT and the field gradient was about 4 nT/cm after compensation, which are limited by the resolution and the sampling rate of the sensors.

In addition, we experimentally achieved magnetic field compensation while the apparatus was rotating. This method does well in compensating for various types of interference simultaneously and quieting an environmental magnetic field without shielding. It can achieve consistent high performance for various types of interference at different frequencies. It is believed that this system will have promising applications in atomic magnetometers, electron microscopes, and atomic clocks.

SUPPLEMENTARY MATERIAL

See the supplementary material for the theory behind the passive eddy-current shielding of an AC magnetic field, the simultaneous compensation of the magnetic fields in the y and z directions, the electronic noise produced by the compensation system, the phase of the 50-Hz field noise in the environment, the compensation of magnetic fields with higher frequencies, the acquisition of a signal of interest from external noise, and the LabVIEW codes of our method.

AUTHORS' CONTRIBUTIONS

K.X. and L.W. contributed equally to this work.

ACKNOWLEDGMENTS

DATA AVAILABILITY

The data that support the findings of this study are available within this article and its supplementary material.

REFERENCES

[1] D. Sheng, S. Li, N. Dural, and M. V. Romalis, Phys. Rev. Lett. **110**, 160802 (2013).

[2] S.-K. Lee, K. L. Sauer, S. J. Seltzer, O. Alem, and M. V. Romalis, Appl. Phys. Lett. **89**, 214106 (2006).

[3] I. M. Savukov, S. J. Seltzer, and M. V. Romalis, J. Magn. Reson. **185**, 214 (2007).

[4] G. Liu, X. Li, X. Sun, J. Feng, C. Ye, and X. Zhou, J. Magn. Reson. **237**, 158 (2013).

[5] X. Wang, M. Zhu, K. Xiao, J. Guo, and L. Wang, J. Magn. Reson. **307**, 106580 (2019).

[6] S. Xu, M. H. Donaldson, A. Pines, S. M. Rochester, D. Budker, and V. V. Yashchuk, Appl. Phys. Lett. **89**, 224105 (2006).

[7] M. P. Ledbetter, V. M. Acosta, S. M. Rochester, D. Budker, S. Pustelny, and V. V. Yashchuk, Phys. Rev. A **75**, 023405 (2007).

[8] V. Gerginov, F. C. S. da Silva, and D. Howe, Rev. Sci. Instrum. **88**, 125005 (2017).

[9] C. Deans, L. Marmugi, and F. Renzoni, Rev. Sci. Instrum. **89**, 083111 (2018).

[10] G. Bevilacqua, V. Biancalana, P. Chessa, and Y. Dancheva, Appl. Phys. B **122**, 103 (2016).

[11] S. J. Seltzer and M. V. Romalis, Appl. Phys. Lett. **85**, 4804 (2004).

[12] I. Hasegawa and A. C. Lilly, Jr., Rev. Sci. Instrum. **40**, 1113 (1969).

[13] P. Treutlein, P. Hommelhoff, T. Steinmetz, T. W. Hänsch, and J. Reichel, Phys. Rev. Lett. **92**, 203005 (2004).

[14] D. Platzek, H. Nowak, F. Giessler, J. Röther, and M. Eiselt, Rev. Sci. Instrum. **70**, 2465 (1999).

[15] C. J. Dedman, R. G. Dall, L. J. Byron, and A. G. Truscott, Rev. Sci. Instrum. **78**, 024703 (2007).

[16] B. Merkel, K. Thirumalai, J. E. Tarlton, V. M. Schäfer, C. J. Ballance, T. P. Harty, and D. M. Lucas, Rev. Sci. Instrum. **90**, 044702 (2019).

[17] L. Botti, R. Buffa, A. Bertoldi, D. Bassi, and L. Ricci, Rev. Sci. Instrum. **77**, 035103 (2006).

[18] J. L. Crassidis, K.-L. Lai, and R. R. Harman, J. Guid. Control Dyn. **28**, 115 (2005).

[19] H. B. Dang, A. C. Maloof, and M. V. Romalis, Appl. Phys. Lett. **97**, 151110 (2010).

[20] G. Bevilacqua, V. Biancalana, A. B.-A. Baranga, Y. Dancheva, and C. Rossi, J. Magn. Reson. **263**, 65 (2016).

[21] C. Krause, D. Drung, M. Götz, and H. Scherer, Rev. Sci. Instrum. **90**, 014706 (2019).